



Electrochemical and Quantum Chemical Calculations of Two Schiff Bases as Inhibitor for Mild Steel Corrosion in Hydrochloric Acid Solution

Nasrin Soltani^{*}, Hosein Salavati, Nahid Rasouli, Mehrnoosh Paziresh, A. Moghadasi
Department of Chemistry, Payame Noor University, P.O. Box 19395-4697, Tehran, I.R. Iran

^{*}E-mail: nasrin_Soltani2056@yahoo.com

Received 17 October 2014; Received in revised form 24 November 2014; Accepted 1 January 2015, Online published: 5 January 2015

ABSTRACT

The corrosion inhibition characteristics of two synthesized Schiff bases, namely N, N'-bis(2-hydroxy-6-nitrobenzaldehyde) benzidine and N, N'-bis(salysylaldehyde) benzidine, on the mild steel corrosion in 2.0 M hydrochloric acid have been investigated by weight loss, potentiodynamic polarization and electrochemical impedance spectroscopy techniques. These studies were carried out at different concentrations, temperatures and durations. Polarization measurements indicate that the two inhibitors act as mixed type inhibitors. The adsorption of inhibitors obeys the Langmuir adsorption isotherm and the thermodynamic parameters (E_a , K_{ads} , ΔG_{ads}^0) were calculated and discussed. Quantum chemical calculations were performed to provide further insight into the inhibition efficiencies determined experimentally.

KEYWORDS: Mild Steel; Schiff Base; Corrosion Inhibition; Electrochemical Impedance Spectroscopy; Polarization.

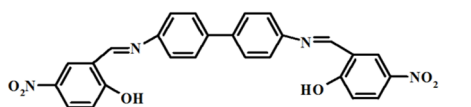
1. INTRODUCTION

Evaluation of mild steel corrosion phenomena has become important especially in acidic media because acids are the most commonly used type of aggressive solutions for pickling, cleaning, descaling and oil well acidization [1]. As acidic media, the use of hydrochloric acid solution is more economical, efficient and trouble-free, compared to mineral acids [2-3]. However, iron and its alloys could be corroded during these applications which result in a waste of resources [4]. To minimize the metal loss during this process, corrosion inhibition programs are required. Several attempts have been made to synthesize various organic and inorganic compounds containing electronegative functional groups (C=O, N-H, O-H and C=S) and electron rich aromatic systems [5-9] and investigated as inhibitors for the corrosion of mild steel [10-12]. In recent years, there is a considerable amount of effort devoted to studying inhibition properties of Schiff bases for metallic corrosion [13-15]. Schiff bases, the condensation products of aldehydes or ketones with amines, are shown to have excellent corrosion inhibition efficiencies when compared to those of the individual constituents [16-18]. Due to the planarity structure and lone pair of electrons present on the N atoms in the presence of -C=N- groups, the Schiff base inhibitors show good corrosion inhibition

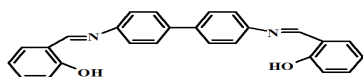
efficiencies [15, 19-25]. The adsorption of these molecules depends mainly on certain physicochemical properties such as functional groups, steric factor, aromaticity, electron density at the donor atoms and π -orbital character of donating electrons [20, 26-29]. Ansari et al. [30] have studied the inhibition efficiency of three Schiff bases of pyridyl substituted triazoles namely (3-phenylallylidene) amino-5-(pyridine-4-yl)-4H-1, 2, 4-triazole-3-thiol (SB-1), 3-mercapto-5 (pyridine-4-yl)-4H-1,2,4-triazole-4-yl) imino) methyl phenol (SB-2) and (4-nitrobenzylidene) amino-5-(pyridine-4-yl)-4H-1,2,4-triazole-3-thiol (SB-3) for mild steel (MS) in 1 M HCl. The inhibition efficiency increases in the following order SB-1 > SB-2 > SB-3 and SB-1 exhibited inhibition performance 96.6 % at 150 mg L⁻¹. 2-((5-mercapto-1,3, 4-thiadiazol-2-ylimino)methyl) phenol Schiff base on mild steel corrosion in 0.5 M HCl solution offered 97% inhibition efficiency [29]. Quantum chemical calculations have been widely used in the study of reaction mechanisms [8]. Effect of hydroxyl group position on adsorption behavior and corrosion inhibition of hydroxybenzaldehyde Schiff bases has been investigated on steel electrode in 1 M HCl by using electrochemical techniques and quantum calculations [19]. The results indicated that IE% of the Schiff bases

was closely related to some of the quantum chemical parameters but with varying degrees/ order. In our previous work we have studied the effects of substitution of methoxy, hydroxyl and chloride groups on the inhibitive effect of N, N'-bis (salicylidene) phenylmethanediamine on mild steel corrosion in hydrochloric acid solution [31].

In this present work, we have studied the inhibition effect of two double Schiff bases (Fig. 1) on the corrosion of mild steel in 2.0 M HCl solution utilizing weight loss measurements, electrochemical techniques and theoretical calculation methods. SB I and SB II are Schiff base compounds whose molecules possess two C=N groups, benzene rings, hydroxyl groups and conjugated double bonds and their only difference is related to the substitution nitro groups on the phenolic ring (in two sides of molecules) in SB I. Because of the many groups which can interact with the surface and with the aim of elucidate the effect of substitution nitro groups on inhibition efficiency, these compounds were selected for study. The adsorption and mechanism of action of these inhibitors are investigated and some of the thermodynamic adsorption parameters such as the equilibrium constant and standard free energy of adsorption in presence of the inhibitors are calculated. The experimental results were associated with a theoretical method and discussed.



SB I: N, N'-bis (2-hydroxy-6-nitrobenzaldehyde) benzidine



SB II: N, N'-bis (salicylaldehyde) benzidine

Fig. 1. The chemical structure of the investigated Schiff bases.

2. EXPERIMENTAL

2.1. Materials

2.1.1. Synthesis of Schiff bases

Two Schiff base derivatives, namely N, N'-bis(2-hydroxy-6-nitrobenzaldehyde) benzidine (SB I) and N, N'-bis(salicylaldehyde) benzidine (SB II) shown in Fig. 1, were synthesized in laboratory according to the following procedures [32]. The structural formula of Schiff base ligands is shown in Fig. 1. The purity of compounds were checked by melting point, elemental analysis, IR spectroscopy and ¹H NMR. (SB I: m.p: 230°C, IR: $\nu(\text{O-H Phenolic})$ (3378 cm^{-1}), $\nu(\text{C=N Azomethine})$, Anal. calcd.: C, 75.83; H, 6.94; N, 8.04. Found: C, 74.80; H, 7.06; N, 8.30%) ($\nu(\text{C=N Azomethine})$ (1611 cm^{-1}), $\nu(\text{C-O phenolic})$ (1450 cm^{-1}), $\nu(\text{-NO}_2 \text{ Nitro group})$ (1380, 1550 cm^{-1}), ¹H NMR/DMSO/ δ ppm: the proton signals at 3.35, 6.9-7.9 and 9.1 ppm are due to the

solvent, aromatic protons and azomethine (-CH=N-) proton respectively, the proton signal around 13 ppm for phenolic (-OH) proton.), (SB II: m.p: 210°C, IR: $\nu(\text{O-H Phenolic})$ (3380 cm^{-1}), $\nu(\text{C=N Azomethine})$ (1614 cm^{-1}), $\nu(\text{C-O phenolic})$ (1460 cm^{-1}) and Anal. calcd.: C, 70.12; H, 6.11; N, 7.40. Found: C, 72.50; H, 7.00; N, 7.50%,), ¹H NMR/DMSO/ δ ppm: The proton signals at 3.35, 6.6-8.5 and 8.78 ppm are due to the solvent, aromatic protons and azomethine (-CH=N-) proton respectively, the proton signal around 9.4 ppm for phenolic (-OH) proton.

2.1.2. Electrodes and Chemicals

Corrosion tests were performed on mild steel samples with the chemical composition (wt.%) of: C (0.027), Si (0.0027), P (0.009), Al (0.068), Mn (0.340), S (0.007), Nb (0.003), Cu (0.007), Ni (0.030), Ti (0.003), Cr (0.008), V (0.003) and Fe (balance). The test specimens were cut into 1 cm \times 1 cm \times 0.1 cm sizes. For the weight loss measurements, a 2 mm diameter small hole was drilled near the upper edge of the specimen to accommodate a suspension hook. While for electrochemical study, each mild steel coupon was soldered on one surface with an insulated copper wire and carefully coated with epoxy resin, leaving the other surface (which had a surface area of 1 cm^2) exposed for corrosion studies. The exposed metal surface was then abraded with different grades of emery papers 200, 400, 800, 1000 and 1500, respectively. It was then washed with double distilled water. The corrosion tests were performed in 2.0 M HCl solution in the absence and presence of various concentrations of Schiff bases ranging from 0.01 mM to 1.00 mM. The HCl solution was prepared by dilution of an analytical grade HCl solution (37%) with distilled water.

2.2. Weight loss measurements

Weight loss experiments were carried out at different immersion times at 25°C. Before immersion in the test solutions with or without the inhibitor, the samples were abraded with different emery paper (grade 200, 400, 800, 1000 and 1500), ultrasonically cleaned in distilled water, rinsed with acetone and finally dried. The weight loss of steel in 2.0 M HCl solution (in $\text{mg cm}^{-2} \text{ h}^{-1}$) with and without the addition of inhibitors were determined at different immersion times at 25°C by weighing the cleaned samples before and after hanging the coupon into 50 ml of the solution. In order to get good reproducibility, experiments were carried out in triplicate and corrosion rate calculated from average weight loss are reported.

2.3. Electrochemical studies

The electrochemical measurements were carried out using an AUTOLAB PGSTAT 35 model potentiostat-galvanostat. A three-electrode cell, consisting of steel working electrode (WE), a platinum counter electrode (CE) and a saturated silver-silver chloride (Ag/AgCl) electrode as a reference electrode, was used for measurements. All experiments were performed in

atmospheric condition without stirring. Before electrochemical measurements, the mild steel electrode was immersed into the corrosive solutions for 1 h in order to establish a steady-state open circuit potential (E_{ocp}). Then, EIS and potentiodynamic polarization measurements were carried out subsequently. After measuring the open circuit potential, potentiodynamic polarization curves were obtained with a scan rate of 0.5 mV s^{-1} in the potential range from -500 to $+500$ mV relative to the E_{ocp} . In order to investigate the mechanism of inhibition and calculate activation energies of corrosion process, polarization curves were obtained at various temperatures ($25\text{--}65^\circ\text{C}$) in the absence and presence of 1.0 mM inhibitors. For this propose, the temperature was adjusted to $25\text{--}65^\circ\text{C}$ using TAMSON model T1000 thermostat. Electrochemical impedance spectroscopy (EIS) measurements were carried out at the open circuit potential (E_{ocp}) after a stationary state was achieved in the frequency range from 100 kHz to 0.1 Hz and AC voltage amplitude of 5 mV peak to peak. Polarization data and impedance data were analyzed using GPES electrochemical software and FRA software respectively.

2.4. Surface analysis

The surface morphology of the mild steel samples after immersion in HCl solution with and without inhibitor, coated by a film of 50 nm of gold by sputtering, was investigated by SEM using a PHILIPS model XL30 microscope.

2.5. Quantum chemical study

The molecular structure has been fully geometrically optimized by B3LYP (Becke 3 term with Lee, Yang, Parr Exchange) model of density functional theory (DFT) for the gas phases with 6-311G**basis using Gaussian 03 software package. The following calculated quantum chemical parameters, such as the population of total charge density, the highest occupied molecular orbital energy (EHOMO) and the lowest unoccupied molecular orbital energy (ELUMO), energy gap ($\Delta E = \text{EHOMO} - \text{ELUMO}$) and dipole moment (μ) were considered. The molecular dynamics (MD) simulations were performed using the Materials Studio 4.0 software (Accelrys, Inc.). Calculations were carried out in a 12×8 supercell using the COMPASS force field and the Smart algorithm with NVE (microcanonical) ensemble, a time step of 1 fs and simulation time 5 ps . Temperature was fixed at 350 K . The system was quenched every 250 steps.

3. RESULTS AND DISCUSSIONS

3.1. Weight loss measurements

Corrosion inhibition performance of organic inhibitors can be evaluated by using weight loss method. This method of monitoring corrosion rate is useful because of its simple application and reliability [33]. The corrosion rate (v) was calculated from the following equation:

$$v = \frac{(m_1 - m_2)}{(S \times t)} \quad (1)$$

where m_1 and m_2 are the initial and final mass of the samples in mg, S is the total surface area of specimens in cm^2 and t is the exposure time in h. With the calculated corrosion rate, the inhibition efficiency and surface coverage (θ) of each concentration of inhibitor for the corrosion of mild steel was obtained by using the following equations:

$$\eta_w(\%) = \frac{(v_0 - v)}{v_0} \times 100 \quad (2)$$

$$\theta = \frac{(v_0 - v)}{v_0} \quad (3)$$

where v_0 and v are the corrosion rates of the specimen in 2 M hydrochloric acid without and with the addition of inhibitor, respectively.

Weight loss of mild steel in 2.0 M HCl in the absence and presence of various concentrations of the Schiff bases was determined after 2, 4, 6, 8 and 24 h of immersion in 2.0 M HCl and in the absence and presence of various concentrations of the Schiff bases and the results are shown in Table 1. From Table 1, it is observed that in the presence of both Schiff bases, corrosion rate of mild steel decreased on increasing concentration. This behavior could be attributed to the increase in adsorption of Schiff bases at the metal/solution interface on increasing its concentration. The order of inhibition efficiency decreased as follows: SBI > SBII. The effect of immersion time at 25°C on the corrosion rates (v) and the η_w of Schiff bases at different concentration are shown in Fig. 2.

It can be concluded from Fig. 2 that both Schiff bases inhibit the corrosion of mild steel for all immersion times. At each concentration, η_w remains constant for different immersion time and suggests the formation of persistent film on the metal surface. This indicates that both Schiff bases are good corrosion inhibitors for mild steel in 2.0 M HCl.

3.2. Open circuit potential (OCP) curves

It is important to provide steady state conditions before accomplishment the potentiodynamic polarization and impedance measurements. Steady state conditions were reached after 1 h in this study. Fig. 3 represents the variation of the OCP of the steel electrode with time in 2.0 M HCl solution in absence and presence of various concentrations of Schiff bases at 25°C . In blank solution, the initial OCP was -0.567 V and this value becomes almost constant around -0.539 V after 1500 s . Fig. 2 shows that, the addition of Schiff bases to the HCl solution shifts the OCP towards positive values at all of the studied concentrations, although there was not a specific relation between E_{corr} and inhibitors concentration. It is observed that the change in OCP of the blank solution is the rapidest relative to the various concentrations of Schiff bases. This evidence may reveal that the dissolution action of mild steel is delayed by inhibitors. The potentiodynamic polarization and impedance measurements were performed after the attainment of the steady state OCP.

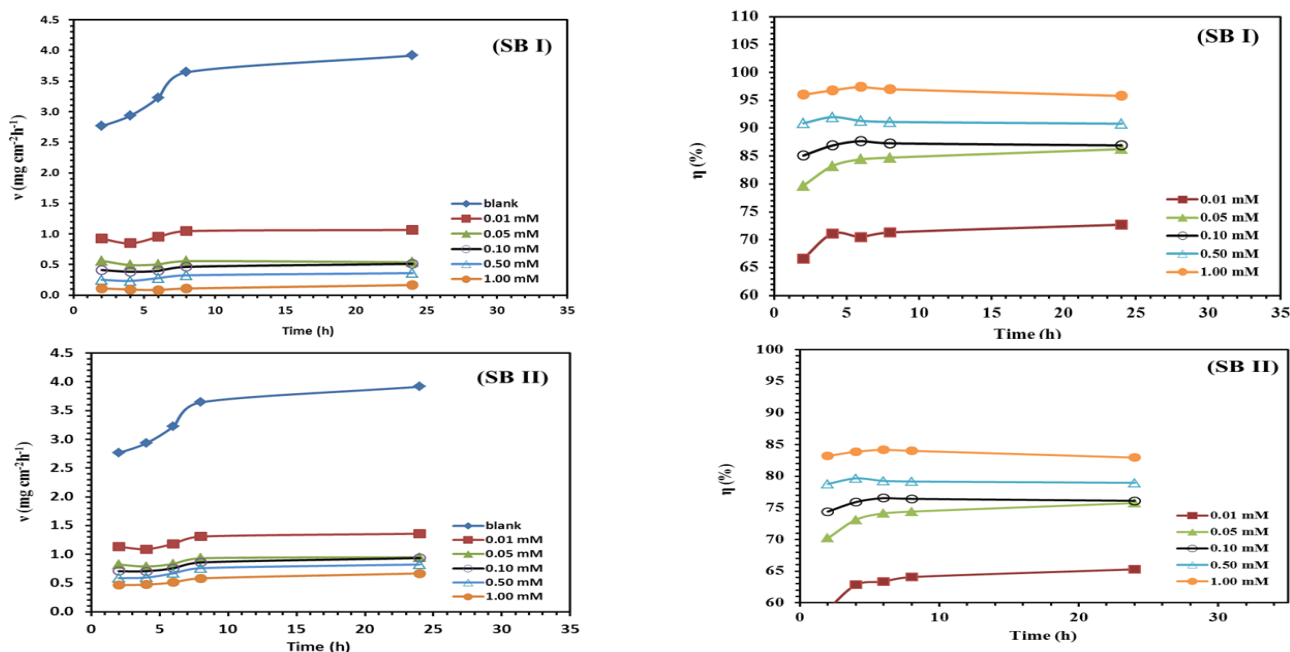


Fig. 2. Relationship between corrosion rate (v) and inhibition efficiency (η_w) with the immersion time in the absence and presence of different concentrations of Schiff bases in 2.0 M HCl at 25 °C.

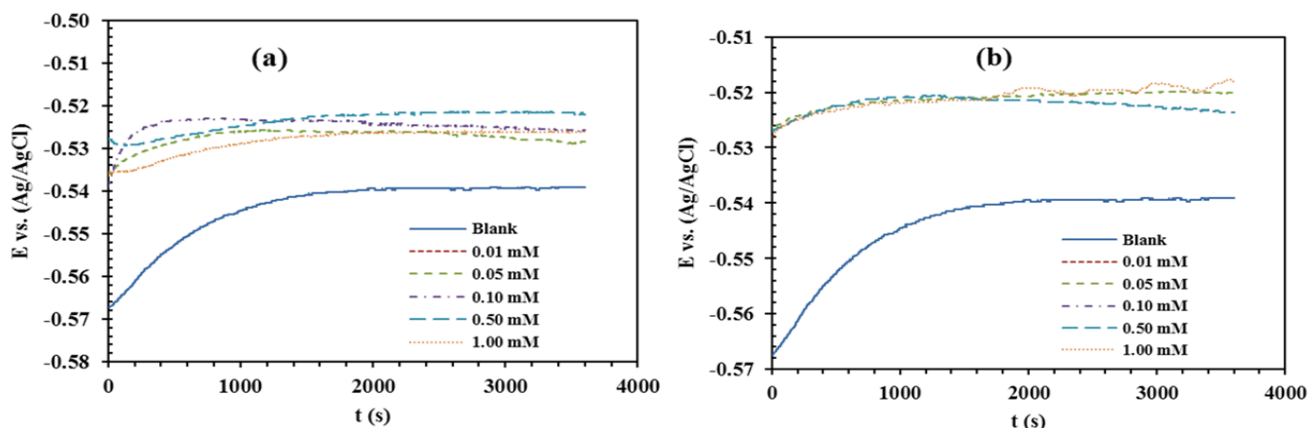


Fig. 3. Variation of the open-circuit potential as a function of time recorded for mild steel electrode in 2.0 M HCl solutions without and with various concentrations of Schiff bases at 25 °C.

Table 1. Weight loss results of mild steel corrosion in 2.0 M HCl with addition of various concentrations of Schiff bases and in various immersion times.

inhibitor	C (mM)	2h		4h		6h		8h		24 h	
		v^a	θ	v	θ	v	θ	v	θ	v	θ
	Blank	2.76	-	2.93	-	3.22	-	3.64	-	3.92	-
SBI	0.01	0.92	0.67	0.85	0.71	0.95	0.71	1.05	0.71	1.07	0.73
	0.05	0.56	0.8	0.49	0.83	0.50	0.84	0.56	0.85	0.54	0.86
	0.10	0.41	0.85	0.38	0.87	0.40	0.88	0.46	0.87	0.51	0.87
	0.50	0.25	0.91	0.23	0.92	0.28	0.91	0.33	0.91	0.36	0.91
	1.00	0.11	0.96	0.09	0.97	0.09	0.97	0.11	0.97	0.17	0.96
SB II	0.01	1.13	0.59	1.09	0.63	1.18	0.63	1.31	0.64	1.36	0.65
	0.05	0.82	0.7	0.79	0.73	0.83	0.74	0.93	0.74	0.95	0.76
	0.10	0.71	0.74	0.71	0.76	0.76	0.77	0.86	0.76	0.93	0.76
	0.50	0.59	0.79	0.60	0.8	0.67	0.79	0.76	0.79	0.82	0.79
	1.00	0.46	0.83	0.47	0.84	0.51	0.84	0.58	0.84	0.67	0.83

^a ($\text{mg cm}^{-2} \text{h}^{-1}$).

3.3. Potentiodynamic polarization measurements

The potentiodynamic polarization profiles of mild steel electrode in 2.0 M HCl solutions in the absence and presence of inhibitors are shown in Fig. 4 (a, b) as Tafel plots. The values of associated electrochemical parameters, i.e., corrosion potential (E_{corr}), corrosion current density (I_{corr}), cathodic Tafel slopes (b_c) and percentage inhibition efficiency (η_p (%)) values were calculated from polarization curves and listed in Table 2. The inhibition efficiency η_p (%) was calculated from polarization measurements according to the relation given below:

$$\eta_p(\%) = \left(\frac{I_{\text{corr}} - I'_{\text{corr}}}{I_{\text{corr}}} \right) \times 100 \quad (4)$$

where I_{corr} and I'_{corr} are uninhibited and inhibited corrosion current densities, respectively. From Fig. 4, it is clear that the presence of corrosion inhibitors causes a prominent decrease in the corrosion rate i.e. shifts

both anodic and cathodic curves to lower values of current densities. Namely, both cathodic and anodic reactions are drastically retarded by corrosion inhibitor in 2.0 M HCl [34]. Inspection of Table 2 reveals that I_{corr} decreases considerably in the presence of both Schiff bases and decreases with increasing concentration of inhibitors. Correspondingly, η_p increases with the inhibitor concentration. η_p of 1.00 mM of SB I and SB II reaches up to a maximum of 95.8% and 83.9%, respectively. This is in good agreement with the range of the inhibition efficiency values obtained from weight loss measurements. Table 2 shows a slight change in anodic and cathodic Tafel slopes for all of inhibited solutions in all concentrations. This means that the presence of inhibitor in the test solution does not modify the process mechanism and act as adsorptive inhibitor, retarding both cathodic and anodic reaction by

Table 2. Electrochemical polarization parameters for mild steel in 2.0 M HCl containing different concentrations of Schiff bases.

Inhibitor	C (mM)	$-E_{\text{corr}}$	$-b_c$	b_a	I_{corr} ($\mu\text{A cm}^{-2}$)	θ	η_p (%)
		vs. Ag/AgCl (mV)	(mV dec ⁻¹)				
Blank	—	536	106	71	397.00	-	-
SB I	0.01	527	105	69	140.00	0.648	64.82
	0.05	523	103	65	83.93	0.789	78.90
	0.10	523	104	75	61.44	0.845	84.50
	0.50	522	100	79	38.76	0.903	90.35
	1.00	527	99	69	13.70	0.958	95.83
SB II	0.01	521	103	72	171.07	0.570	57.02
	0.05	518	107	69	122.23	0.693	69.29
	0.10	517	102	75	105.14	0.636	73.67
	0.50	517	108	76	87.01	0.781	78.10
	1.00	519	101	73	62.83	0.829	82.93

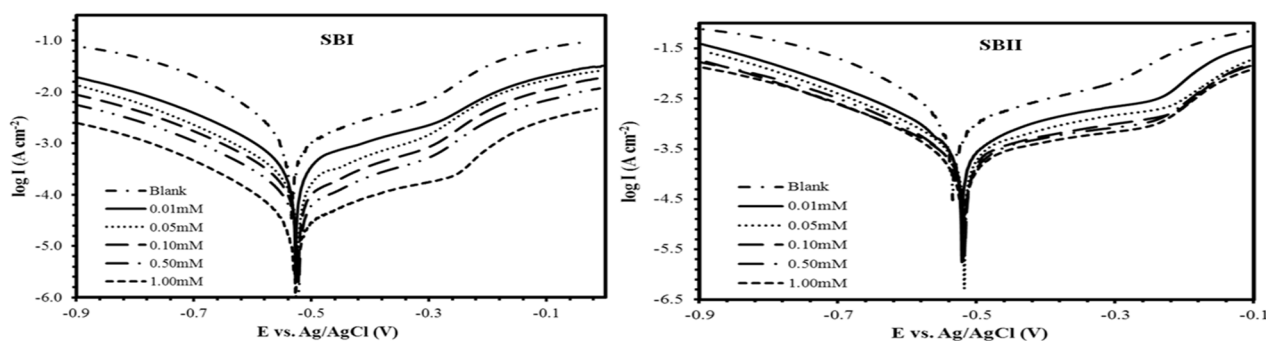


Fig. 4. Polarization curves for mild steel in 2.0 M HCl in the absence and presence of different concentrations of Schiff bases at 25°C.

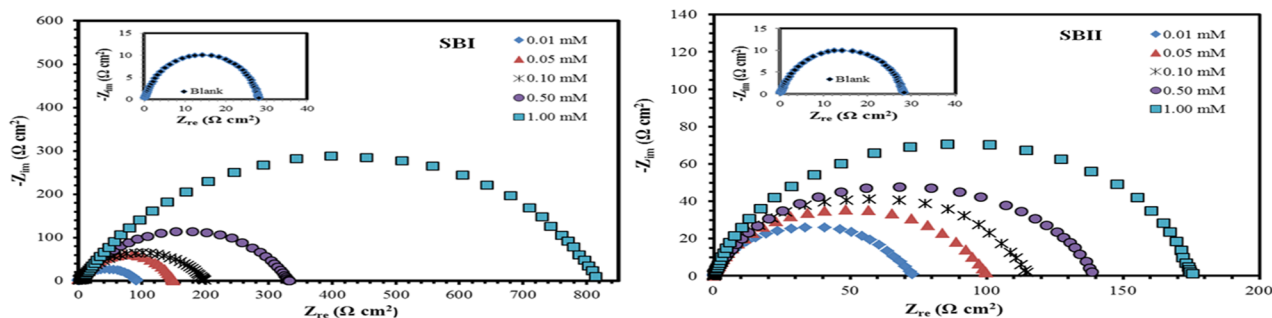


Fig. 5. Nyquist plot for mild steel in 2.0 M HCl in the absence and presence of different concentrations of Schiff base at 25 °C.

Table 3. Impedance parameters with corresponding inhibition efficiency for the corrosion of mild steel in 2.0 M HCl at different concentrations of Schiff bases.

Inhibitor	C(mM)	R_s	R_{ct} ($\Omega \text{ cm}^2$)	Y_0 ($\mu\Omega^{-1} \text{ s}^n \text{ cm}^{-2}$)	n	C_{dl} ($\mu\text{F cm}^{-2}$)	$\eta_{EIS}(\%)$
Blank	—	0.20	28.3	75.9	0.79	26.9	-
SB I	0.01	0.43	91.5	55.8	0.81	21.2	68.8
	0.05	0.21	150.4	28.6	0.83	17.4	81.1
	0.10	0.21	199.4	24.2	0.85	8.5	85.7
	0.50	0.31	331.0	16.2	0.89	7.9	91.4
	1.00	0.99	814.0	11.4	0.90	7.2	96.5
SB II	0.01	0.15	72.9	69.4	0.79	23.7	61.1
	0.05	0.22	100.1	63.2	0.80	21.4	71.8
	0.10	0.34	115.0	52.3	0.81	19.8	75.6
	0.50	0.67	138.7	41.2	0.84	18.3	79.6
	1.00	0.72	175.0	33.5	0.85	15.7	83.7

blocking the active sites [35]. From Table 2 also can find that the corrosion potential of both inhibitors changed slightly towards the positive direction. But as electrode potential displacement is lower than 85 mV these compounds can be classified as mixed corrosion inhibitors [36].

3.4. Electrochemical impedance spectroscopy (EIS)

The inhibition efficiencies of Schiff bases on mild steel were examined by electrochemical impedance spectroscopy. The impedance spectra of mild steel in 2.0 M HCl solution in the absence and presence of five different concentrations of Schiff bases were recorded. Fig. 5 shows the impedance spectra in Nyquist format. As seen from the plots, the impedance response contains a single capacitive loop, corresponding to one time constant, whose size increased by increasing the concentration of Schiff bases. The capacitive loop was attributed to a faradic process involving a charge transfer resistance in parallel with double-layer capacitance element [37-38]. This indicated that the charge transfer takes place at electrode/solution interface, and the transfer process controls corrosion reaction and the presence of inhibitor does not change the mechanism of steel dissolution [39]. The simplest fitting is represented by Randles equivalent circuit. The equivalent circuit diagram and the Impedance

parameters are given in Fig. 6 and Table 3, respectively. The circuit consists of parallel combination of the charge-transfer resistance (R_{ct}) and the constant phase element (CPE), both in series with the solution resistance (R_s). In order to give a more accurate fit to the experimental results the constant phase element (CPE) was used for fitting instead of a double layer capacitance (C_{dl}). In other words, due to the distribution of the relaxation times as a result of inhomogeneities present at a micro- or nano- level, such as the surface roughness/porosity, adsorption, or diffusion the use of a CPE is required [40-41].

As it can be seen from the Fig. 5, the Nyquist plots are slightly depressed as semi-circular shapes because of the roughness and other inhomogeneities of mild steel surface resulting in a phenomenon called "dispersing effect" [42, 43].

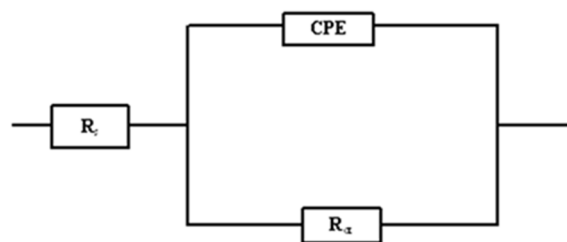


Fig. 6. Equivalent circuit model for the studied inhibitors.

The impedance of a constant phase element is described by the expression [43]:

$$Z_{CPE} = [Y_0(j\omega)^n]^{-1} \quad (5)$$

where Y_0 is the magnitude of the CPE, n the CPE exponent (phase shift), ω the angular frequency ($\omega = 2\pi f$, where f is the AC frequency), and j here is the imaginary unit. When the value of n is 1, the CPE behaves like an ideal double-layer capacitance (C_{dl}). The correction of capacity to its real values is calculated from

$$C_{dl} = Y_0(\omega_{max})^{n-1} \quad (6)$$

where ω_{max} is the angular frequency at which the imaginary part of the impedance has a maximum. The data obtained from fitted spectra are listed in Table 3. Table 3 shows that the R_s values are very small in comparison with the R_{ct} values. The R_{ct} values increased with inhibitor concentrations which demonstrate that the inhibitor with the formation of a protective layer on the electrode surface and making a barrier for mass and charge-transfer prevents the corrosion reaction effectively [44]. It is also observed that C_{dl} decreases with increase in concentration. This decrease in double layer capacitance can happen by a decrease in local dielectric constant and/or an increase in the thickness of the electrical double layer [45]. According to the Helmholtz model, the change of these values can be related to the gradual replacement of water molecules by inhibitor molecules on the surface and consequently, leads to decrease in the number of active sites necessary for the corrosion reaction [40]. Inhibitor efficiency can be estimated by charge transfer resistance according to the following equation [12]:

$$\eta_{EIS}\% = \frac{R_{ct} - R_{ct}^0}{R_{ct}} \times 100 \quad (7)$$

Where R_{ct}^0 and R_{ct} are the charge transfer resistances in the absence and the presence of inhibitors, respectively. The values of η_{EIS} (%) Schiff bases are in quite good agreement with the results obtained from weight loss and polarization measurements.

3.5. Effect of temperature and kinetic parameters

To evaluate the activation energy of the corrosion process and investigate the effect of temperature, potentiodynamic polarization measurements were performed in the temperature range of 25–65°C in 2.0 M HCl solution in the absence and presence of 1.0 mM of Schiff bases. Fig. 7 presents polarization curves for mild steel electrode in 2.0 M HCl, with and without 1.0 mM of Schiff bases at 35–65°C. The obtained corrosion rates and $\eta_p\%$ are given in Table 4 and show when temperature increases, in the absence and presence of inhibitor, the I_{corr} increases. From Table4,

it is also obvious that the η_p (%) slightly increase in the temperature range 25–65°C.

In order to calculate apparent activation energy E_a for the corrosion process, Arrhenius equation was used [37]:

$$r = A \exp\left(-\frac{E_a}{RT}\right) \quad (8)$$

where A is a constant, T the absolute temperature and r is the rate of metal dissolution reaction which is directly related to corrosion current density (I_{corr}) [46]. The apparent activation energy of the corrosion reaction in presence and absence of the inhibitors could be calculated by plotting $\ln I_{corr}$ with $1/T$ from the slopes of the straight lines in Fig. 8.

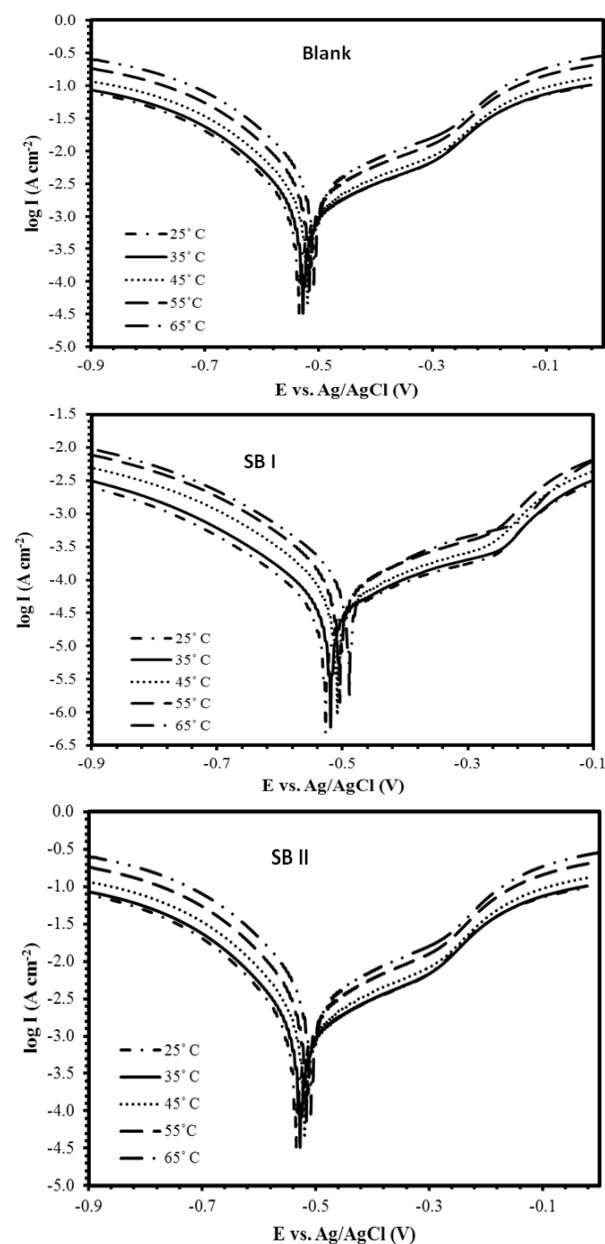
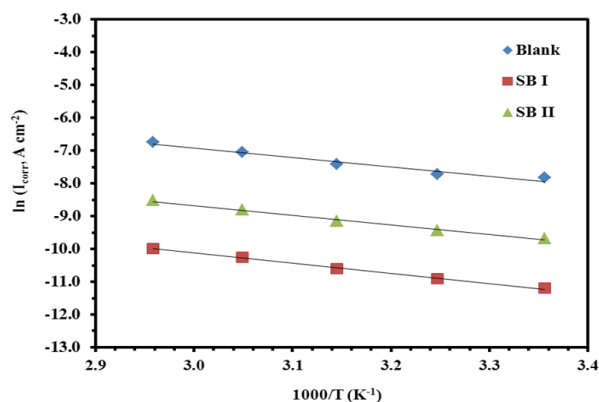


Fig. 7. Effect of temperature on polarization curves of mild steel corrosion rate in free and inhibited acid solutions.

Table 4. Polarization parameters and corresponding inhibition efficiency for the corrosion of the mild steel in 2.0 M HCl without and with addition of 1 mM of Schiff bases at different temperatures.

Inhibitor	Temperature (°C)	$-E_{corr}$ (mV)	I_{corr} ($\mu\text{A cm}^{-2}$)			η_P (%)
				$-b_c$ (mV dec $^{-1}$)	b_a	
Blank	25	536	397.0	76	59	-
	35	528	440.6	64	54	-
	45	520	600.4	58	66	-
	55	517	875.2	86	58	-
	65	509	1190.1	69	80	-
SB I	25	527	13.7	73	65	95.83
	35	519	18.2	112	56	95.92
	45	510	24.7	92	59	95.9
	55	506	35.0	92	59	96.04
	65	489	46.2	105	62	96.14
SB II	25	519	62.8	83	57	82.93
	35	513	79.4	105	63	82.97
	45	506	105.1	92	59	83.04
	55	503	148.9	52	81	83.08
	65	487	199.9	109	51	83.16

**Fig. 8.** Arrhenius plots of mild steel in 2.0 M HCl in absence and presence of 1 mM of different inhibitors.

All the linear regression coefficients are close to 1, indicating that the steel corrosion in hydrochloric acid can be elucidated using the kinetic model. The apparent activation energy obtained for the corrosion process was 27.4, 25.8 and 24.5 kJ mol $^{-1}$ for uninhibited HCl, in the presence of SB I and SB II, respectively. The relationships between the temperature dependence of percentage η_P of an inhibitor and the E_a can be classified into three groups according to temperature effects

- (i) η_P decreases with increase in temperature, E_a (inhibited solution) $>$ E_a (uninhibited solution);
- (ii) η_P does not change with temperature, E_a (inhibited solution) = E_a (uninhibited solution);

(iii) η_P increases with increase in temperature, E_a (inhibited solution) $<$ E_a (uninhibited solution).

For two inhibitors, E_a (inhibited solution) $<$ E_a (uninhibited solution), which further confirm η_P increases with increase in temperature.

The reason of decrease of the activation energy in the presence of inhibitor has been explained in different ways in literature Putilova showed that at higher temperatures, the surface covered by inhibitor increases and rate determining step of the metal dissolution becomes the diffusion through the film of corrosion products and inhibitor [47].

3.6. Adsorption isotherm considerations

As mentioned in previous sections the adsorption of inhibitors on steel surface occurs through water molecules replacement with the organic inhibitors molecules and cause the number of active sites necessary for the corrosion reaction was reduced. The adsorption provides the information about the interaction among the adsorbed molecules themselves as well as their interaction with the electrode surface [34]. So, it is essential to know the mode of adsorption and the adsorption isotherm. Attempts were made to fit to various isotherms including Frumkin, Langmuir, Temkin, Freundlich, Bockris–Swinkels and Flory–Huggins isotherms. The fractional surface coverage θ , at different concentrations of Schiff bases in acidic

chloride solutions was determined from corresponding electrochemical polarization data according to following equation [48]:

$$\theta = \frac{I_{corr} - I'_{corr}}{I_{corr}} \quad (9)$$

and the surface coverage values θ are represented in Table 2. For the studied inhibitors, it is found that the best fit was obtained from the Langmuir isotherm (Fig. 9).

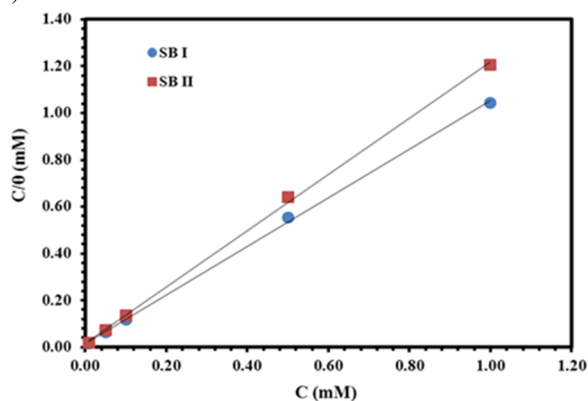


Fig. 9. Langmuir isotherm for adsorption of Schiff bases on the mild steel surface.

According to this isotherm, the surface coverage θ is related to the equilibrium adsorption constant K_{ads} and concentration of inhibitor C via [31]:

$$\frac{C}{\theta} = \frac{1}{K_{ads}} + C \quad (10)$$

The equilibrium constant for adsorption process is related to the free energy of adsorption, ΔG_{ads} and is expressed by following equation [49]:

$$K_{ads} = \frac{1}{55.5} \exp\left(-\frac{\Delta G_{ads}}{RT}\right) \quad (11)$$

where 55.5 is the concentration of water in the solution in mol L⁻¹, R is the universal gas constant (8.314 J K⁻¹ mol⁻¹) and T is the absolute temperature (K).

The values of adsorption constant, slope and linear correlation coefficient (R^2) can be obtained from the regressions between C/θ and C , and the results are listed in Table 5. Noticeably, the slope values of C/θ versus C for SB II deviate from 1, which indicates the interaction force among the adsorbed species cannot be neglected [50-51]. While, the slope of the straight line, for SB I is close to unity which suggests that the interaction of adsorbed species is negligible [50]. The thermodynamics parameters derived from Langmuir adsorption isotherms for the studied compounds, are also given in Table 5. The negative values of ΔG_{ads} and the higher values of K_{ads} indicate the spontaneity of adsorption process and they are characteristic of strong interaction and stability of the adsorbed layer with the steel surface. The negative values of ΔG_{ads}^0 - 20 kJ

mol⁻¹ or lower are attributed to the electrostatic interaction between the charged molecules and the charged metal (physisorption). Furthermore, those around -40 kJ mol⁻¹ or higher involve charge sharing or transfer from organic molecules to the metal surface to form a coordinate type of bond (chemisorption) [30, 52]. The value of -40 kJ mol⁻¹ is usually adopted as a threshold value between chemisorption and physisorption [53]. According the calculated values of the ΔG_{ads}^0 , in Table 5 we conclude that both physical and chemical processes may be occur in the adsorption of the compounds.

Table 5. Linear correlation coefficient, R^2 , slope, equilibrium constant, K_{ads} , and the free energy of adsorption, ΔG_{ads}^0 of Schiff bases for mild steel in 2.0 M HCl solution at 25 °C.

Inhibitor	Slope	K_{ads} (M ⁻¹)	R^2	$-\Delta G_{ads}^0$ (kJ mol ⁻¹)
SB I	1.04	1.00×10^5	0.9992	38.5
SB II	1.20	5.00×10^4	0.9992	36.7

3.7. Scanning electron microscopy (SEM)

The SEM images are taken and observed in order to support our findings. Fig. 10 shows the SEM images of mild steel surface. It can be seen from Fig. 10a that the mild steel samples before immersion seems smooth and appears some abrading scratches on the surface. After immersion in uninhibited 2.0 M HCl solution for 6 h, the mild steel surface appears an aggressive attack of the corroding medium as shown in Fig. 10b. As can be seen from Fig. 10c and d, there was much less damage on the surface of the mild steel with SB I and SB II which further confirms the inhibition ability.

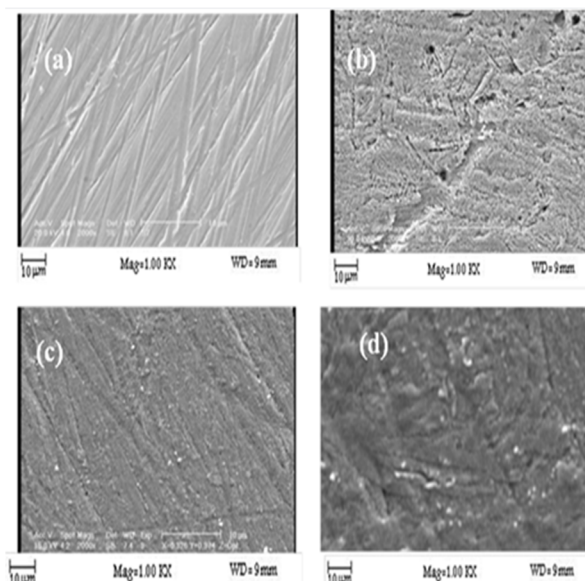


Fig. 10. SEM micrographs of steel samples after 6 h immersion period (a) before corrosion, (b) 1 M HCl, (c) 2.0 M + 1 mM of SB I and (d) 2.0 M + 1 mM of SB II.

3.8. Quantum chemical studies

The effectiveness of an inhibitor is related to its spatial molecular structure as well as with its molecular electronic structure [54-55]. Thus, some quantum chemical calculations were performed here to throw more light on the adsorption mode of studied Schiff bases. The density functional theory (DFT) is one of the most important theoretical models used in explaining the science of solids and chemistry. B3LYP, a version of the DFT method that uses Becker's three parameter functional (B3) and includes a mixture of HF with DFT exchange terms associated with the gradient corrected correlation functional of Lee, Yang and Parr (LYP) [56], was used in this research to carry out quantum calculations. Fig. 11 shows the optimized molecular structures and the frontier molecule orbital density distribution of the studied Schiff bases obtained using DFT at B3LYP/6-311G** level of theory.

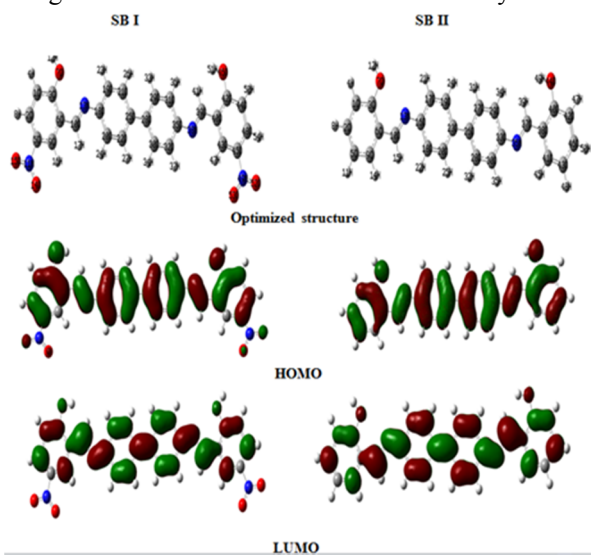


Fig. 11. Frontier molecule orbital density distributions of the two molecules.

The calculated quantum chemical parameters such as the energies of the molecular orbitals, E_{HOMO} (highest occupied molecular energy) and E_{LUMO} (lowest unoccupied molecular orbital energy), $\Delta E = E_{LUMO} - E_{HOMO}$ (energy of the gap), μ (dipole moment) are listed in Table 6. A high E_{HOMO} value expresses intrinsic electron donating tendency to an appropriate acceptor, i.e. any molecule with lower HOMO energy and empty molecular orbital while, E_{LUMO} , the energy of the lowest unoccupied molecular orbital signifies the electron receiving tendency of a molecule. Lower values of the energy difference, ΔE , will cause a good inhibition efficiency, as the energy to remove an electron from the highest-energy occupied molecular orbital will be low [57]. Inspection of Table 6 showed that E_{HOMO} and E_{LUMO} of the two molecules obey the

order: SB I > SB II. Obviously, the sequence of E_{LUMO} is not in accordance with the order of experimental inhibition efficiency, which indicates that there is a complex nature of interactions involved in the corrosion inhibition process [3]. In addition, for the dipole moment (μ), the lower value will favor the more accumulation of inhibitor molecules on the metallic surface [58].

Table 6. Quantum chemical parameters of used Schiff bases obtained from B3LYP/6-311G** method.

Inhibitor	E_{HOMO} (eV)	E_{LUMO} (eV)	ΔE (eV)	μ (D)
SB I	-0.2040	-0.0830	0.1211	3.2441
SB II	-0.2220	-0.1025	0.1196	9.462

The atoms and groups that may interact with the electrode surface were obtained from geometry of the inhibitor as well as the nature of its frontier molecular orbitals derived from quantum chemical calculations. Both Schiff bases are same in structure and the only their differences is substitutions on the benzene rings in two sides of molecules. From optimized geometry of Schiff bases Fig. 11, it can be observed that both molecules have planar structure. Thus, the adsorption of studied Schiff bases on steel surface would take place through C=N groups, benzene rings, hydroxyl groups and nitro groups (in SB I). The frontier molecular orbitals are analyzed in Fig. 11 and it can be seen that HOMO and LUMO orbitals for both Schiff bases are localized and saturated around all parts of the molecule. Hence it should be expecting flat-lying adsorption orientation of Schiff bases on the metal surface. For a better understanding, the molecular dynamics simulations were performed to study the adsorption behavior of the two Schiff base molecules on the Fe (110) surface. Fig. 12 shows the on-top and side views of the optimized Fe-molecule adsorption structures for single molecules of SB I and SB II. The molecules can be seen to maintain a flat-lying adsorption orientation on the Fe surface in order to maximize contact, as expected from the delocalization of the electron density around the molecules. The corresponding interaction energies (E_{inter}) were computed using the relationship:

$$E_{inter} = E_{total} - (E_{Fe} + E_{molecule}) \quad (12)$$

E_{total} , E_{Fe} and E_{mol} denote the energies of the adsorbed Fe/molecule couple, the Fe slab and the molecule respectively, which were obtained by averaging the energies of the five structures of the lowest energy. The E_{inter} for SB I and SB II are -190.46, and -162.91 kcal.mol⁻¹, respectively. The trend of E_{inter} (SB II < SB I) suggests stronger interaction of SB I with the Fe

surface, which is in good agreement with the experimental results.

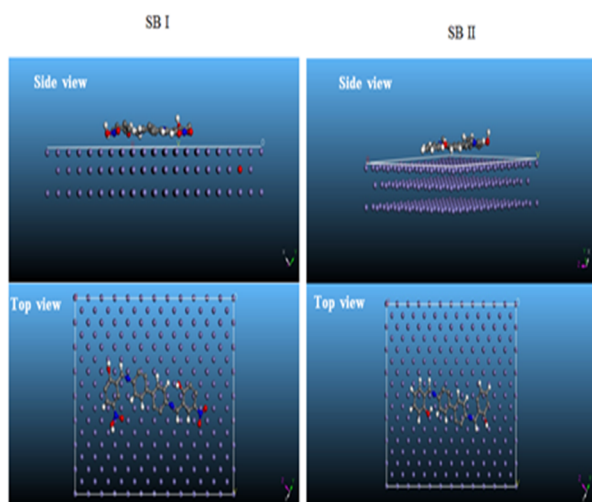
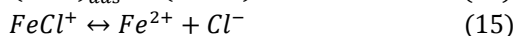
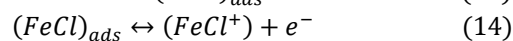
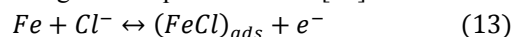


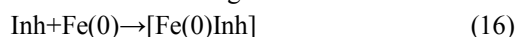
Fig. 12. Equilibrium adsorption configurations of Schiff bases on Fe (110) surface obtained by molecular dynamic simulations. Top: side view, bottom: top view.

3.9. Mechanism of adsorption and inhibition

An explanation of the mechanism of inhibition requires full knowledge of the interaction between the protective organic inhibitor and the metal surface. Due to the activation effect of chloride ions, the pitting corrosion of the blank specimen under HCl proceeded according to the equations 13-15 [59]:



The two Schiff base molecules exist as protonated form in HCl solution, which is in equilibrium with the corresponding molecular form (Inh). In the pitting area of surface, Cl^- anions are first adsorbed onto the positively charged metal surface. Therefore, $InhH^+$ reacts with Fe (II) and forms a thick and protective $[FeClInhH^+]$ complex. For specimens in the inhibited HCl solutions, the $[Fe(0)Inh]$ complex is formed at the flat area via the following reaction:



Inhibitor quickly reacts with Fe (0) and forms a strong protective layer in the noncorroded area. The layer is very thin and is probably a single monolayer. Finally, caustic ions were blocked by the protective film and the steel was effectively protected from corrosion.

4. CONCLUSIONS

The inhibition efficiency of both Schiff bases increased with increasing of its concentration but it's slightly decreases with an increase in temperature range 25–65°C. Double layer capacitances decrease with respect

to HCl solution when inhibitors are added. This fact can be explained by adsorption of inhibitors on the steel surface. Polarization curves demonstrate that the examined Schiff bases behave as mixed type inhibitor. The adsorption of both Schiff bases on mild steel surface follow the Langmuir adsorption isotherm model. The high K_{ads} values indicate a strong interaction between the inhibitors and the mild steel surface and the ΔG_{ads}^0 values suggest that this interaction may occur by both physical and chemical adsorption. The inhibition ability of both Schiff bases follows the order: SB I > SB II, which has been confirmed by the experimental measurements and theoretical calculation measurements. Molecular dynamics simulation results reveal that both Schiff bases adsorb on the iron surface in a nearby flat manner.

REFERENCES

- [1] A. Adewuyi, A. Göpfert and T. Wolff, Succinyl amide gemini surfactant from Adenopus breviflorus seed oil: A potential corrosion inhibitor of mild steel in acidic medium, *Ind. Crop. Prod.* 52 (2014) 439-449.
- [2] X. Li, S. Deng, H. Fu and T. Li, Adsorption and inhibition effect of 6-benzylaminopurine on cold rolled steel in 1.0 M HCl, *Electrochim. Acta* 54 (2009) 4089-4098.
- [3] B. Xu, W. Yang, Y. Liu, X. Yin, W. Gong and Y. Chen, Experimental and theoretical evaluation of two pyridinecarboxaldehyde thiosemicarbazone compounds as corrosion inhibitors for mild steel in hydrochloric acid solution, *Corros. Sci.* 78 (2014) 260-268.
- [4] R. Solmaz, Investigation of adsorption and corrosion inhibition of mild steel in hydrochloric acid solution by 5-(4-Dimethylaminobenzylidene) rhodanine, *Corros. Sci.* 79 (2014) 169-176.
- [5] A. Döner, R. Solmaz, M. Özcan and G. Kardaş, Experimental and theoretical studies of thiazoles as corrosion inhibitors for mild steel in sulphuric acid solution, *Corros. Sci.* 53 (2011) 2902-2913.
- [6] C.M. Goulart, A. Esteves-Souza, C.A. Martinez-Huitle, C.J.F. Rodrigues, M.A.M. Maciel and A. Echevarria, Experimental and theoretical evaluation of semicarbazones and thiosemicarbazones as organic corrosion inhibitors, *Corros. Sci.* 67 (2013) 281-291.
- [7] B.P. Markhali, R. Naderi, M. Mahdavian, M. Sayebani and S.Y. Arman, Electrochemical impedance spectroscopy and electrochemical noise measurements as tools to evaluate corrosion

- inhibition of azole compounds on stainless steel in acidic media, *Corros. Sci.* 75 (2013) 269-279.
- [8] D. Özkır, K. Kayakırılmaz, E. Bayol, A.A. Gürten and F. Kandemirli, The inhibition effect of Azure A on mild steel in 1 M HCl. A complete study: Adsorption, temperature, duration and quantum chemical aspects, *Corros. Sci.* 56 (2012) 143-152.
- [9] B. Qian, J. Wang, M. Zheng and B. Hou, Synergistic effect of polyaspartic acid and iodide ion on corrosion inhibition of mild steel in H₂SO₄, *Corros. Sci.* 75 (2013) 184-192.
- [10] G. Moretti, F. Guidi and F. Fabris, Corrosion inhibition of the mild steel in 0.5 M HCl by 2-butyl-hexahydropyrrolo[1,2-b][1,2]oxazole, *Corros. Sci.* 76 (2013) 206-218.
- [11] I.B. Obot, E.E. Ebenso and M.M. Kabanda, Metronidazole as environmentally safe corrosion inhibitor for mild steel in 0.5 M HCl: Experimental and theoretical investigation, *J. Environ. Chem. Engin.* 1 (2013) 431-439.
- [12] S. Pournazari, M.H. Moayed and M. Rahimizadeh, In situ inhibitor synthesis from admixture of benzaldehyde and benzene-1,2-diamine along with FeCl₃ catalyst as a new corrosion inhibitor for mild steel in 0.5 M sulphuric acid, *Corros. Sci.* 71 (2013) 20-31.
- [13] M.A. Hegazy, H.M. Ahmed and A.S. El-Tabei, Investigation of the inhibitive effect of p-substituted 4-(N,N,N-dimethyldodecylammonium bromide)benzylidene-benzene-2-yl-amine on corrosion of carbon steel pipelines in acidic medium, *Corros. Sci.* 53 (2011) 671-678.
- [14] N.A. Negm, Y.M. Elkholy, M.K. Zahran and S.M. Tawfik, Corrosion inhibition efficiency and surface activity of benzothiazol-3-ium cationic Schiff base derivatives in hydrochloric acid, *Corros. Sci.* 52 (2010) 3523-3536.
- [15] R. Solmaz, Investigation of the inhibition effect of 5-((E)-4-phenylbuta-1,3-dienylideneamino)-1,3,4-thiadiazole-2-thiol Schiff base on mild steel corrosion in hydrochloric acid, *Corros. Sci.* 52 (2010) 3321-3330.
- [16] A.A. Farag and M.A. Hegazy, Synergistic inhibition effect of potassium iodide and novel Schiff bases on X65 steel corrosion in 0.5 M H₂SO₄, *Corros. Sci.* 74 (2013) 168-177.
- [17] N.A. Negm, E.A. Badr, I.A. Aiad, M.F. Zaki and M.M. Said, Investigation the inhibitory action of novel diquaternary Schiff dibases on the acid dissolution of carbon steel in 1 M hydrochloric acid solution, *Corros. Sci.* 65 (2012) 77-86.
- [18] B. Xu, Y. Liu, X. Yin, W. Yang and Y. Chen, Experimental and theoretical study of corrosion inhibition of 3-pyridinecarbozaldehyde thiosemicarbazone for mild steel in hydrochloric acid, *Corros. Sci.* 74 (2013) 206-213.
- [19] I. Danaee, O. Ghasemi, G.R. Rashed, M. Rashvand Avei and M.H. Maddahy, Effect of hydroxyl group position on adsorption behavior and corrosion inhibition of hydroxybenzaldehyde Schiff bases: Electrochemical and quantum calculations, *J. Mol. Struct.* 1035 (2013) 247-259.
- [20] S.M. Shaban, A. Saied, S.M. Tawfik, A. Abd Elaal and I. Aiad, Corrosion inhibition and biocidal effect of some cationic surfactants based on Schiff base, *J. Ind. Eng. Chem.* 19 (2013) 2004-2009.
- [21] K. Mallaiya, R. Subramaniam, S.S. Srikandan, S. Gowri, N. Rajasekaran and A. Selvaraj, Electrochemical characterization of the protective film formed by the unsymmetrical Schiff's base on the mild steel surface in acid media, *Electrochim. Acta* 56 (2011) 3857-3863.
- [22] N. Negm and M. Zaki, Synthesis and characterization of some amino acid derived Schiff bases bearing nonionic species as corrosion inhibitors for carbon steel in 2N HCl, *J. Disper. Sci. Technol.* 30 (2009) 649-655.
- [23] A.A. Farag and M. Hegazy, Synergistic inhibition effect of potassium iodide and novel Schiff bases on X65 steel corrosion in 0.5 M H₂SO₄, *Corros. Sci.* 74 (2013) 168-177.
- [24] I. Aiad and N.A. Negm, Some corrosion inhibitors based on Schiff base surfactants for mild steel equipments, *J. Disper. Sci. Technol.* 30 (2009) 1142-1147.
- [25] A. Samide and B. Tutunaru, Adsorption and inhibitive properties of a Schiff base for the corrosion control of carbon steel in saline water, *J. Environ. Sci. Heal. A* 46 (2011) 1713-1720.
- [26] C.B.P. Kumar and K.N. Mohana, Corrosion inhibition efficiency and adsorption characteristics of some Schiff bases at mild steel/hydrochloric acid interface, *J. Taiwan Inst. of Chem. Engin.* 5 (2014) 1031-1042.
- [27] J. Liu, Z. Liu, S. Yuan and J. Liu, Synthesis, crystal structures, and spectral characterization of tetranuclear Mn(II) complex with a new Schiff base ligand and molecular dynamics studies on inhibition properties of such Schiff base, *J. Mol. Struct.* 1037 (2013) 191-199.
- [28] E.E. Shehata, M.S. Masoud, E.A. Khalil and A.M. Abdel-Gaber, Synthesis, spectral and electrochemical studies of some Schiff base N₂O₂ complexes, *J. Mol. Liq.* 194 (2014) 149-158.

- [29] R. Solmaz, E. Altunbaş and G. Kardaş, Adsorption and corrosion inhibition effect of 2-((5-mercapto-1,3,4-thiadiazol-2-ylimino)methyl)phenol Schiff base on mild steel, *Mater. Chem. Phys.* 125 (2011) 796-801.
- [30] K.R. Ansari, M.A. Quraishi and A. Singh, Schiff's base of pyridyl substituted triazoles as new and effective corrosion inhibitors for mild steel in hydrochloric acid solution, *Corros. Sci.* 79 (2014) 5-15.
- [31] N. Soltani, M. Behpour, S.M. Ghoreishi and H. Naeimi, Corrosion inhibition of mild steel in hydrochloric acid solution by some double Schiff bases, *Corros. Sci.* 52 (2010) 1351-1361.
- [32] S.S. A. R. Ray, S. Acharya and R. K. Dey, Studies of metal ion uptake behavior of formaldehyde condensed resins of phenolic Schiff bases derived from the reaction of 4,4"-diamino diphenyl and 4,4"-diamino diphenyl methane with o-hydroxy benzaldehyde, *Indian J. Chem. Techn.* 11 (2004) 695-703.
- [33] M.K. Pavithra, T.V. Venkatesha, M.K. Punith Kumar and H.C. Tondan, Inhibition of mild steel corrosion by Rabepazole sulfide, *Corros. Sci.* 60 (2012) 104-111.
- [34] M.A. Hegazy, A.M. Badawi, S.S. Abd El Rehim and W.M. Kamel, Corrosion inhibition of carbon steel using novel N-(2-(2-mercaptoacetoxy)ethyl)-N,N-dimethyl dodecan-1-aminiun bromide during acid pickling, *Corros. Sci.* 69 (2013) 110-122.
- [35] M. Bobina, A. Kellenberger, J.P. Millet, C. Muntean and N. Vaszilcsin, Corrosion resistance of carbon steel in weak acid solutions in the presence of l-histidine as corrosion inhibitor, *Corros. Sci.* 69 (2013) 389-395.
- [36] L. Fragoza-Mar, O. Olivares-Xometl, M.A. Domínguez-Aguilar, E.A. Flores, P. Arellanes-Lozada and F. Jiménez-Cruz, Corrosion inhibitor activity of 1,3-diketone malonates for mild steel in aqueous hydrochloric acid solution, *Corros. Sci.* 61 (2012) 171-184.
- [37] O.E. Barcia and O.R. Mattos, Reaction model simulating the role of sulphate and chloride in anodic dissolution of iron, *Electrochim. Acta* 35 (1990) 1601-1608.
- [38] G. Quartarone, L. Ronchin, A. Vavasori, C. Tortato and L. Bonaldo, Inhibitive action of gramine towards corrosion of mild steel in deaerated 1.0 M hydrochloric acid solutions, *Corros. Sci.* 64 (2012) 82-89.
- [39] X. Li, S. Deng and H. Fu, Allyl thiourea as a corrosion inhibitor for cold rolled steel in H₃PO₄ solution, *Corros. Sci.* 55 (2012) 280-288.
- [40] B.D. Mert, M. Erman Mert, G. Kardaş and B. Yazıcı, Experimental and theoretical investigation of 3-amino-1,2,4-triazole-5-thiol as a corrosion inhibitor for carbon steel in HCl medium, *Corros. Sci.* 53 (2011) 4265-4272.
- [41] D. Risović, S.M. Poljaček, K. Furić and M. Gojo, Inferring fractal dimension of rough/porous surfaces—A comparison of SEM image analysis and electrochemical impedance spectroscopy methods, *Appl. Surf. Sci.* 255 (2008) 3063-3070.
- [42] S. Ramesh and S. Rajeswari, Corrosion inhibition of mild steel in neutral aqueous solution by new triazole derivatives, *Electrochim. Acta* 49 (2004) 811-820.
- [43] F. Zhang, Y. Tang, Z. Cao, W. Jing, Z. Wu and Y. Chen, Performance and theoretical study on corrosion inhibition of 2-(4-pyridyl)-benzimidazole for mild steel in hydrochloric acid, *Corros. Sci.* 61 (2012) 1-9.
- [44] K.F. Khaled, Application of electrochemical frequency modulation for monitoring corrosion and corrosion inhibition of iron by some indole derivatives in molar hydrochloric acid, *Mater. Chem. Phys.* 112 (2008) 290-300.
- [45] M. Özcan and İ. Dehri, Determination of impedance parameters for mild steel/HCl interface using integration method, *Corros. Sci.* 54 (2012) 201-204.
- [46] G. Achary, H.P. Sachin, Y.A. Naik and T.V. Venkatesha, The corrosion inhibition of mild steel by 3-formyl-8-hydroxy quinoline in hydrochloric acid medium, *Mater. Chem. Phys.* 107 (2008) 44-50.
- [47] I. Putilova, S. Balezin and V. Barannik, *Metallic corrosion inhibitors'*, 1960, in, Oxford: Pergamon Press, 1976.
- [48] Sudheer and M.A. Quraishi, Electrochemical and theoretical investigation of triazole derivatives on corrosion inhibition behavior of copper in hydrochloric acid medium, *Corros. Sci.* 70 (2013) 161-169.
- [49] S.M. Abd El Haleem, S. Abd El Wanees, E.E. Abd El Aal and A. Farouk, Factors affecting the corrosion behaviour of aluminium in acid solutions. I. Nitrogen and/or sulphur-containing organic compounds as corrosion inhibitors for Al in HCl solutions, *Corros. Sci.* 68 (2013) 1-13.
- [50] X. Li, S. Deng, H. Fu and X. Xie, Synergistic inhibition effects of bamboo leaf extract/major components and iodide ion on the corrosion of steel in H₃PO₄ solution, *Corros. Sci.* 78 (2014) 29-42.
- [51] G. Mu, X. Li, Q. Qu and J. Zhou, Molybdate and tungstate as corrosion inhibitors for cold rolling

- steel in hydrochloric acid solution, *Corros. Sci.* 48 (2006) 445-459.
- [52] A. Döner, E.A. Şahin, G. Kardaş and O. Serindağ, Investigation of corrosion inhibition effect of 3-[(2-hydroxy-benzylidene)-amino]-2-thioxo-thiazolidin-4-one on corrosion of mild steel in the acidic medium, *Corros. Sci.* 66 (2013) 278-284.
- [53] M. Hosseini, S.F.L. Mertens and M.R. Arshadi, Synergism and antagonism in mild steel corrosion inhibition by sodium dodecylbenzenesulphonate and hexamethylenetetramine, *Corros. Sci.* 45 (2003) 1473-1489.
- [54] I.B. Obot, N.O. Obi-Egbedi and S.A. Umoren, The synergistic inhibitive effect and some quantum chemical parameters of 2,3-diaminonaphthalene and iodide ions on the hydrochloric acid corrosion of aluminium, *Corros. Sci.* 51 (2009) 276-282.
- [55] S. Şafak, B. Duran, A. Yurt and G. Türkoğlu, Schiff bases as corrosion inhibitor for aluminium in HCl solution, *Corros. Sci.* 54 (2012) 251-259.
- [56] C. Lee, W. Yang and R.G. Parr, Development of the Colle-Salvetti correlation-energy formula into a functional of the electron density, *Phys. Rev. B* 37 (1988) 785-789.
- [57] A.Y. Musa, R.T.T. Jalgham and A.B. Mohamad, Molecular dynamic and quantum chemical calculations for phthalazine derivatives as corrosion inhibitors of mild steel in 1 M HCl, *Corros. Sci.* 56 (2012) 176-183.
- [58] K.F. Khaled, Electrochemical investigation and modeling of corrosion inhibition of aluminum in molar nitric acid using some sulphur-containing amines, *Corros. Sci.* 52 (2010) 2905-2916.
- [59] L. Guo, S. Zhu, S. Zhang, Q. He and W. Li, Theoretical studies of three triazole derivatives as corrosion inhibitors for mild steel in acidic medium, *Corros. Sci.* 87 (2014) 366-375.